Supporting Information

Facile in situ fabrication of biomorphic Co_2P-Co_3O_4/rGO/C as efficient electrocatalyst for oxygen reduction reaction

Xingmei Guo,[a] Cheng Qian,[a] Xiaohan Wan,[a] Wei Zhang,[a] Haowei Zhu,[a] Junhao Zhang,*[a] Hongxun Yang,[a] Shengling Lin,[a] Qinghong Kong[b] and Tongxiang Fan*[c]

[a]School of Environmental and Chemical Engineering, Jiangsu University of Science and Technology, Zhenjiang, Jiangsu 212003, China
Email: jhzhang6@just.edu.cn
[b]School of the Environment and Safety Engineering, Jiangsu University, Zhenjiang, Jiangsu 212013, China.
[c]School of Materials Science and Technology, Shanghai Jiaotong University, Shanghai 200240, China
Email: txfan@sjtu.edu.cn

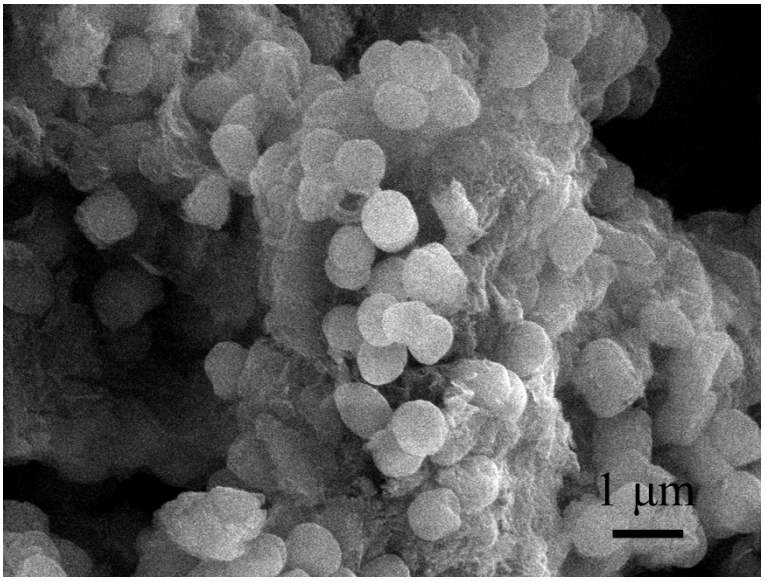

Fig. S1 FESEM image of Streptococcus thermophiles adsorbed with precursor and GO.

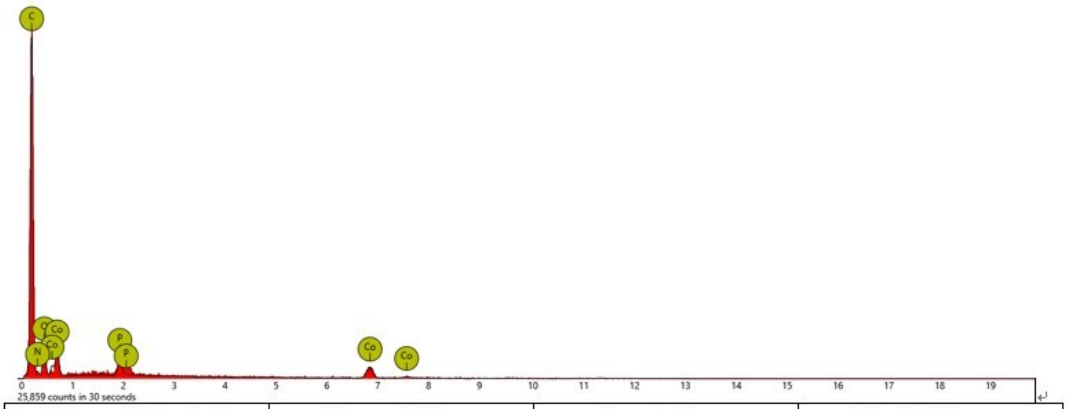

Element Symbol	Element Name	Atomic Conc.	Weight Conc.
C	Carbon	52.49	36.24
O	Oxygen	33.88	31.15
Co	Cobalt	7.20	24.40
N	Nitrogen	3.31	2.67
P	Phosphorus	3.11	5.54

Fig. S2 EDX spectrum and detailed elemental data of Co_2P-Co_3O_4/rGO/C.

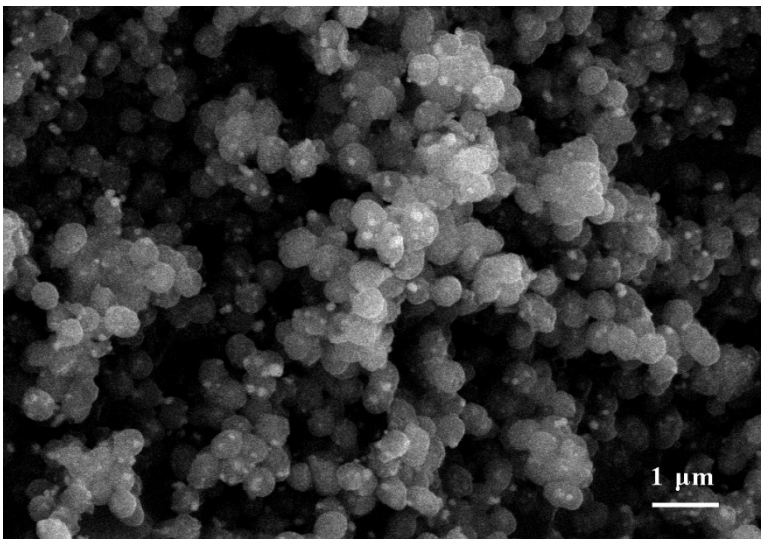

Fig. S3 FESEM image of biomorphic Co_2P-Co_3O_4/C sample.

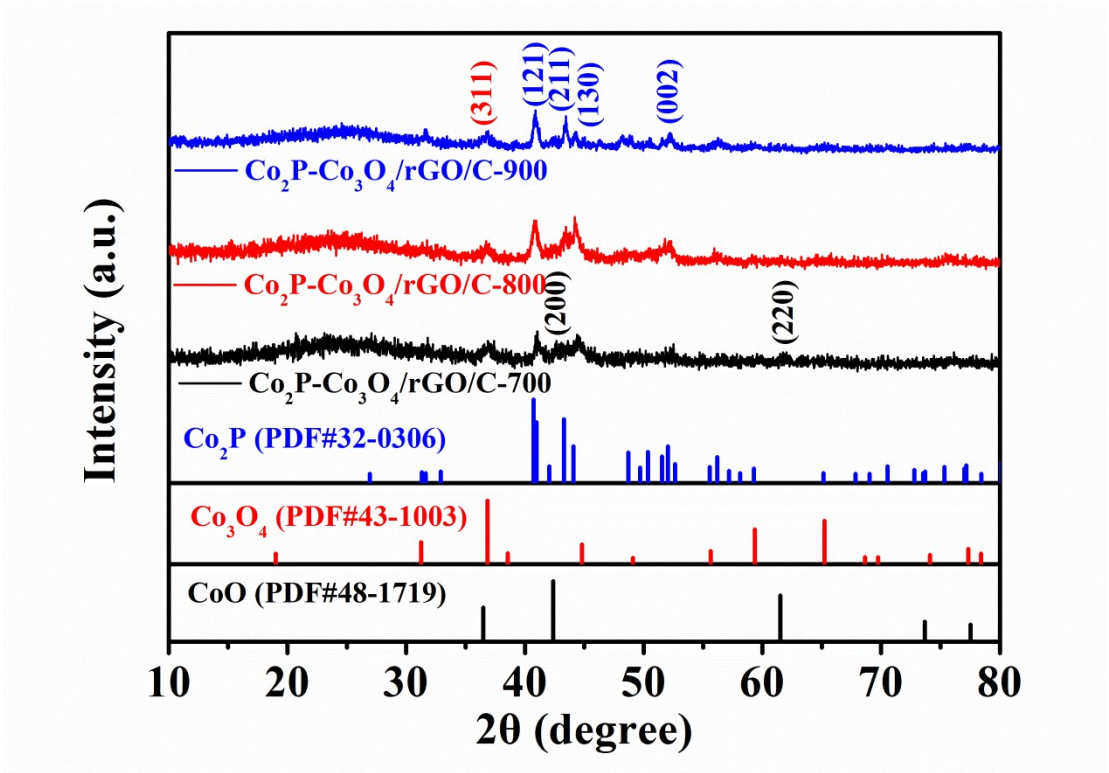

Fig. S4 XRD patterns of Co_2P-Co_3O_4/rGO/C with different calcining temperatures.

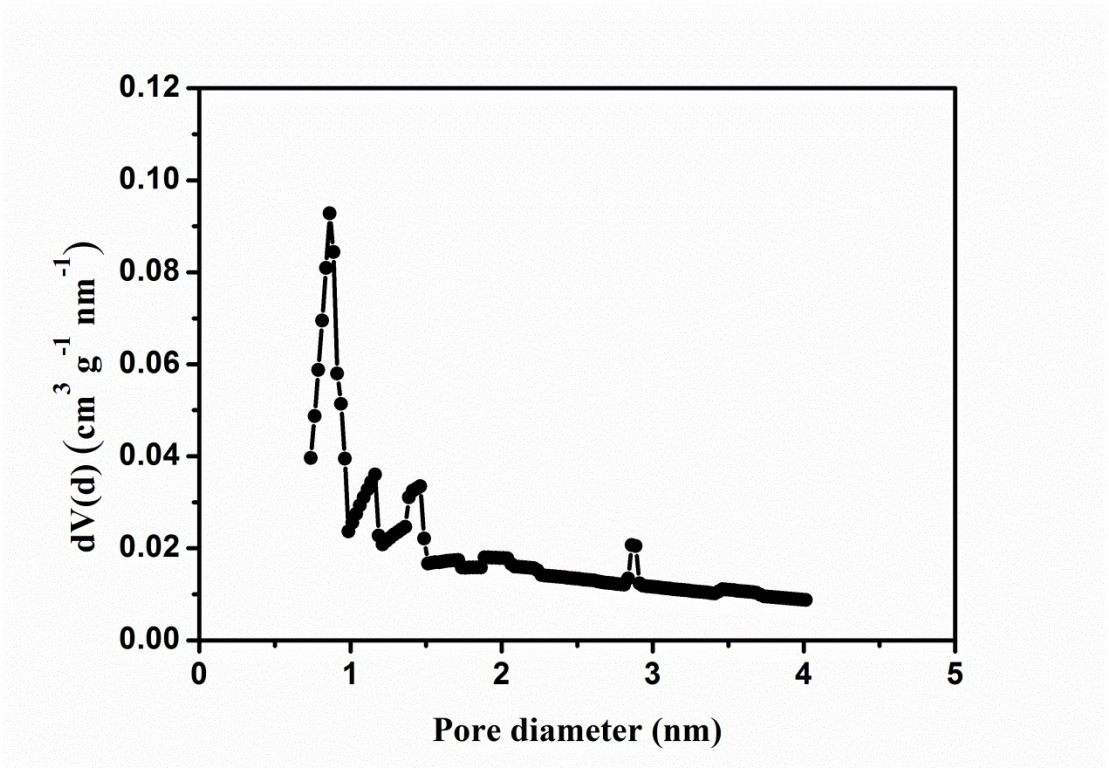

Fig. S5 Micropore size distribution of Co_2P-Co_3O_4/rGO/C calculated through HK method.

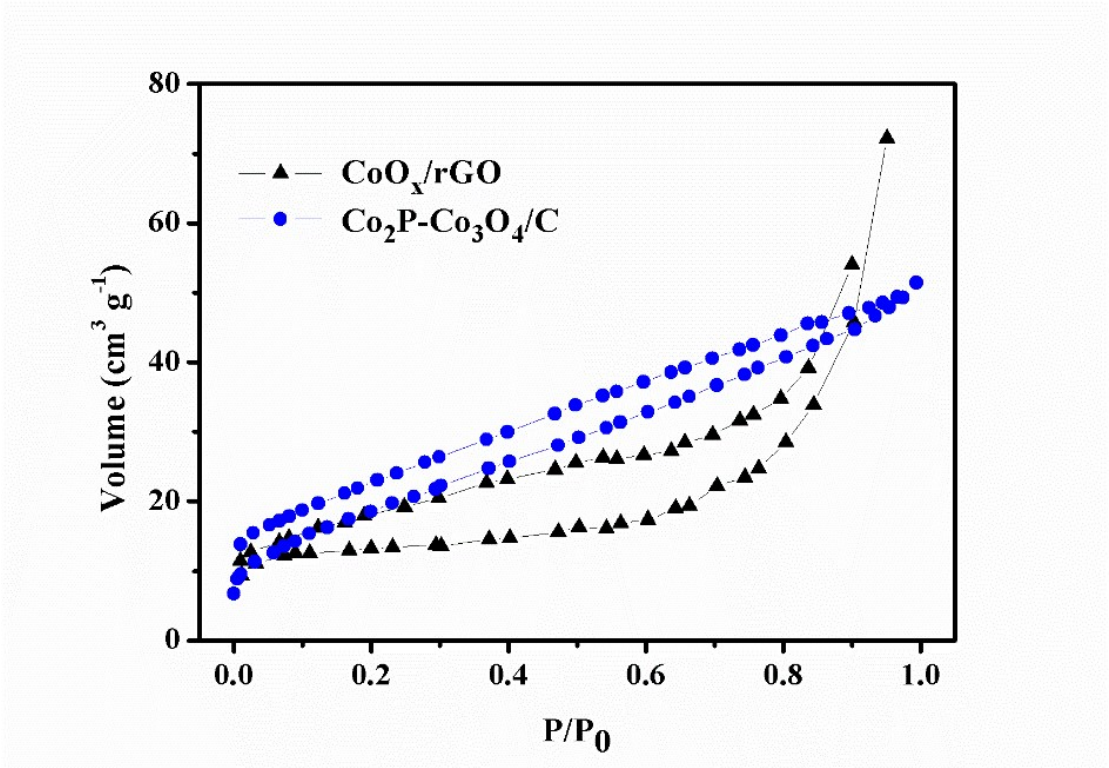

Fig. S6 N_2 adsorption/desorption isotherms of CoO_x/rGO and Co_2P-Co_3O_4/C.

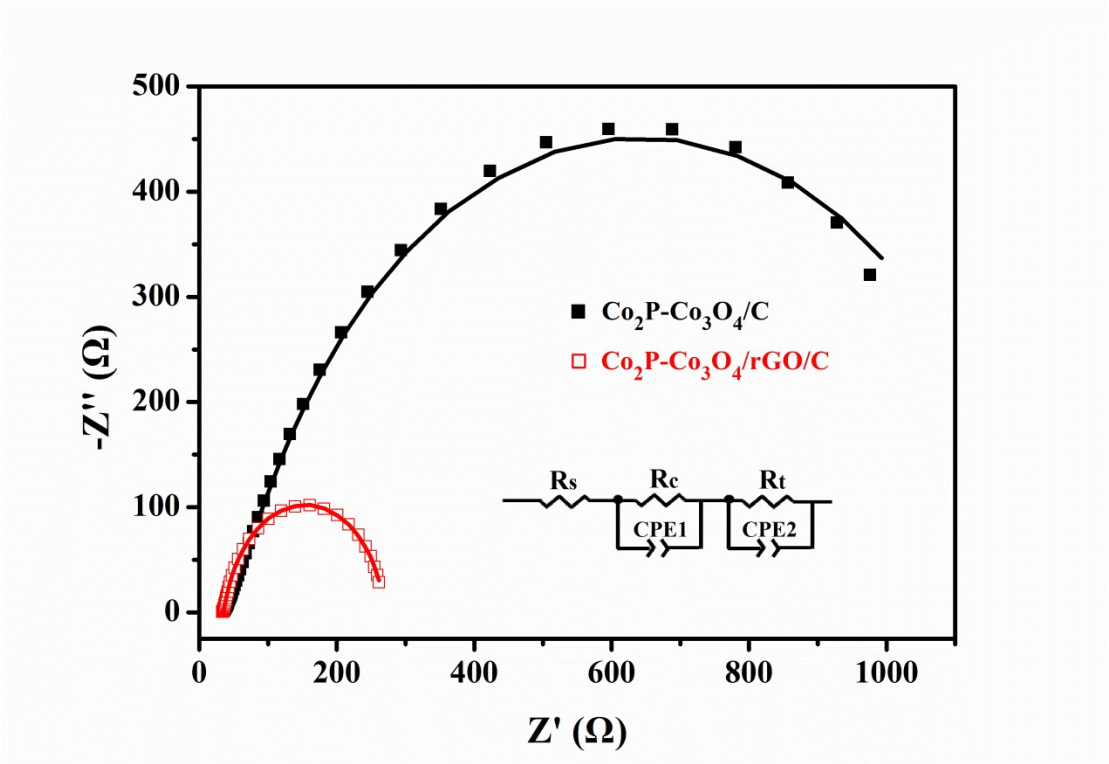

Fig. S7 Actual and fitting Nyquist plots for ORR at 0.85 V vs. RHE on Co_2P-Co_3O_4/C and Co_2P-Co_3O_4/rGO/C. Inset: the equivalent circuit.

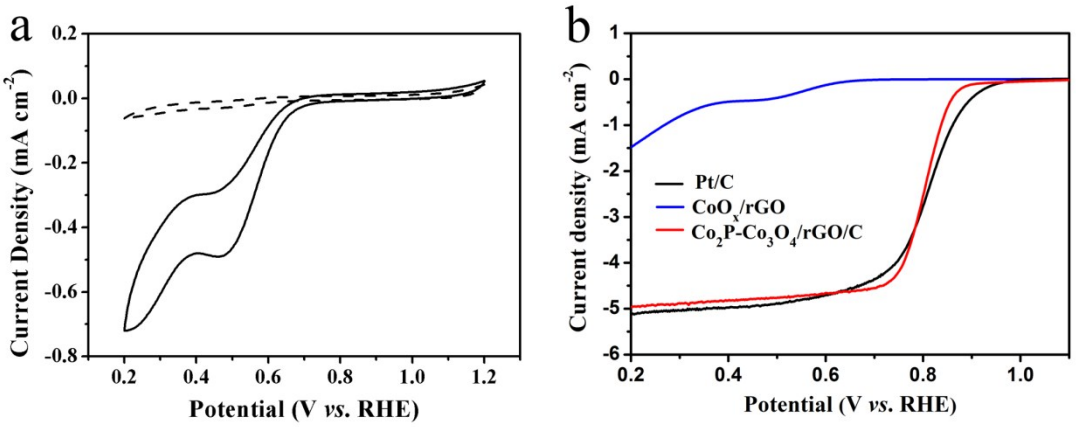

Fig. S8 (a) CV curves of CoO_x/rGO in oxygen (solid line) and nitrogen (dotted line) saturated KOH solution. (b) LSV curves of CoO_x/rGO, Co_2P-Co_3O_4/rGO/C and Pt/C in oxygen saturated KOH solution at a rotation speed of 1600 rpm.

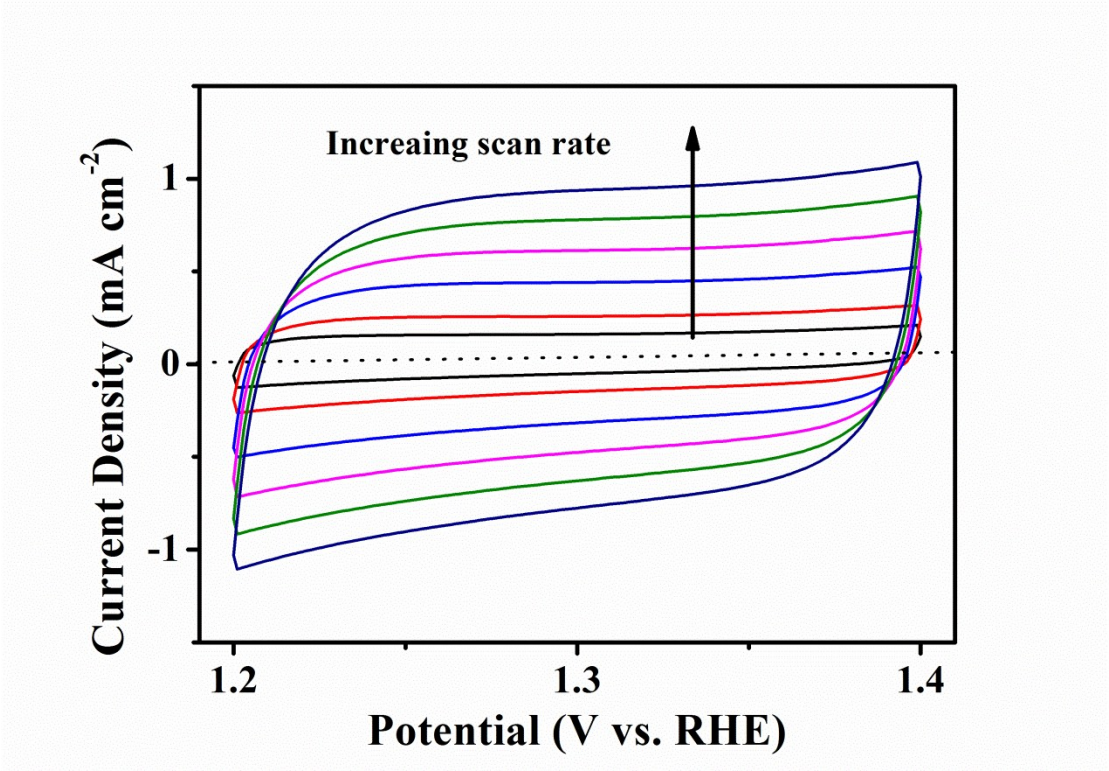

Fig. S9 CV curves of Co_2P-Co_3O_4/rGO/C in the potential range of 1.2-1.4 V vs. RHE with scan rates increasing from 10 to 100 mV s^{-1}.

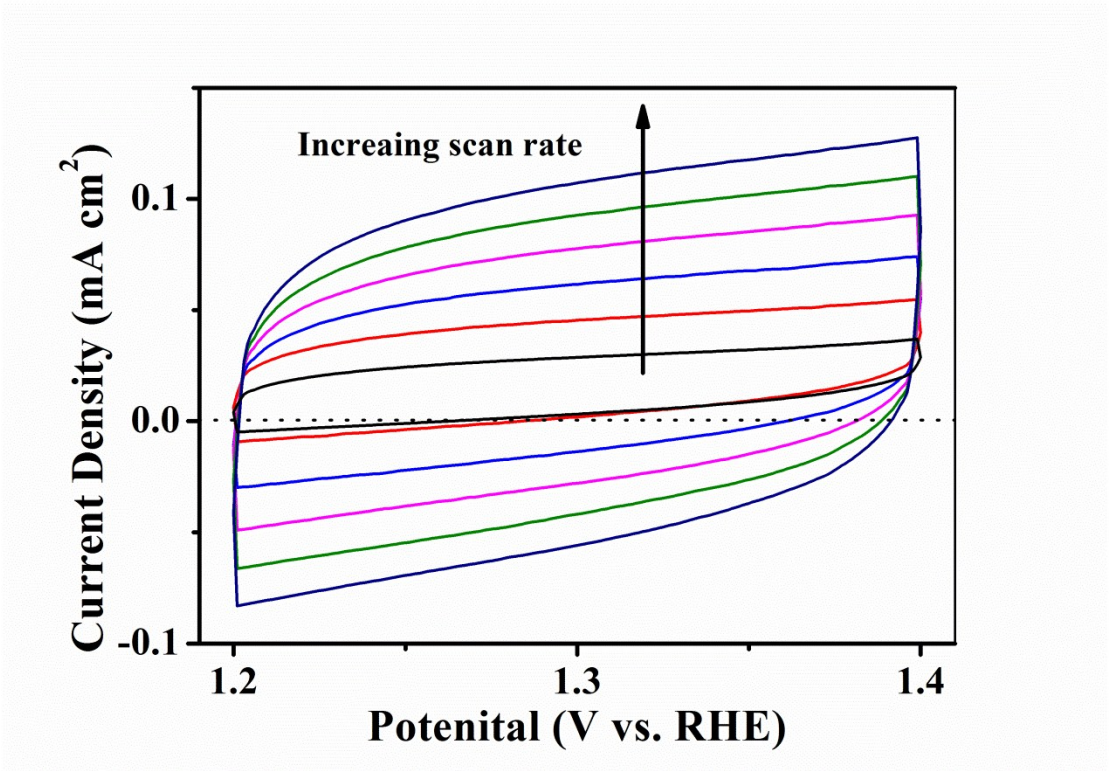

Fig. S10 CV curves of Pt/C in the potential range of 1.2-1.4 V vs. RHE with scan rates increasing from 10 to 100 mV s^{-1}.

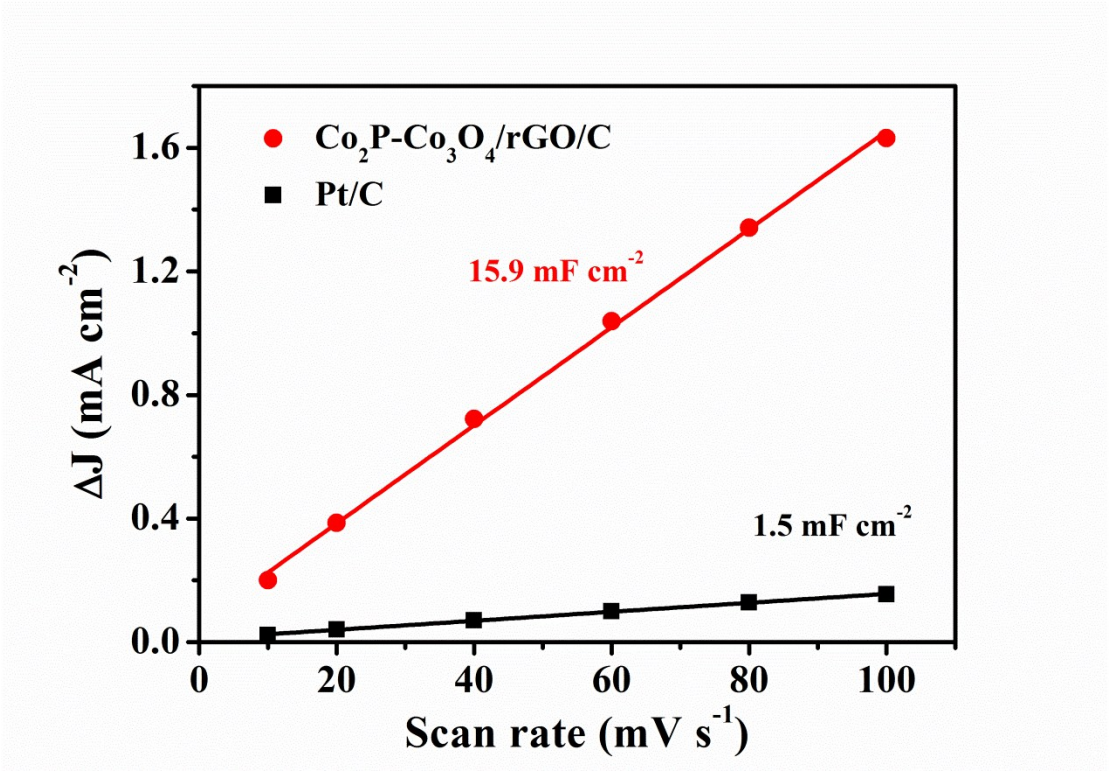

Fig. S11 Current density differenced at 1.35 V vs. RHE as a function of scan rates.

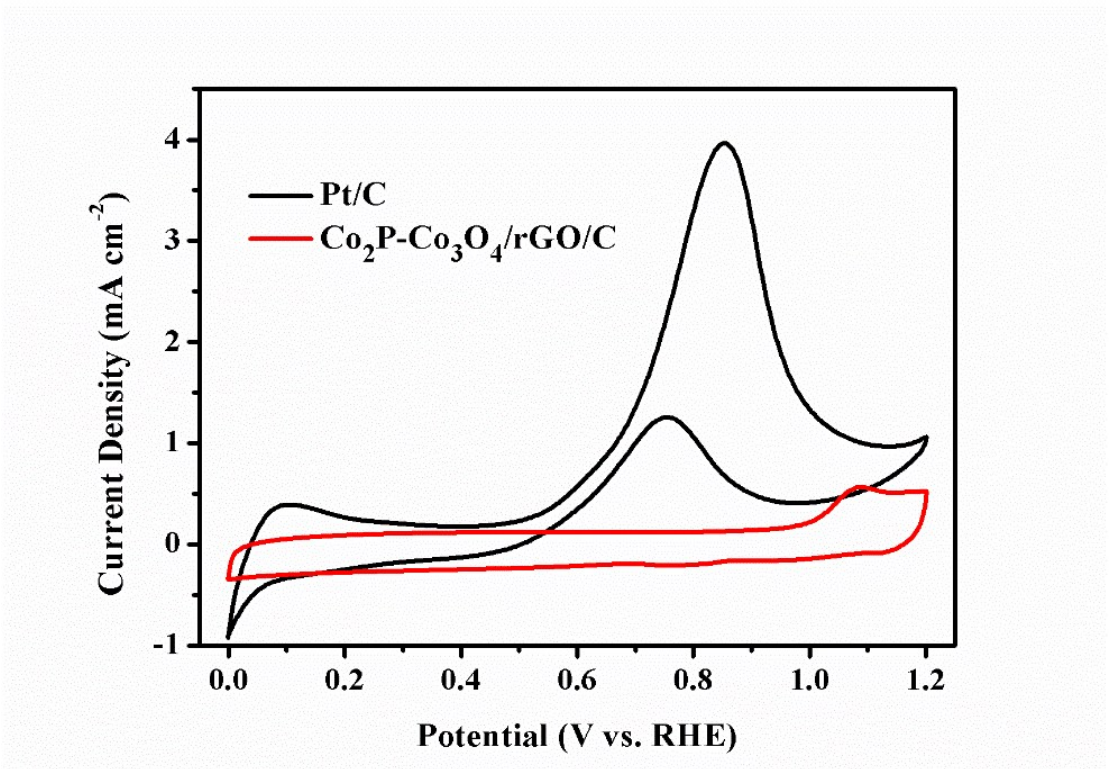

Fig. S12 CV curves of Co_2P-Co_3O_4/rGO/C and Pt/C in 0.1 mol L^{-1} KOH containing 0.1 mol L^{-1} methanol at a scan rate of 50 mV s^{-1}.

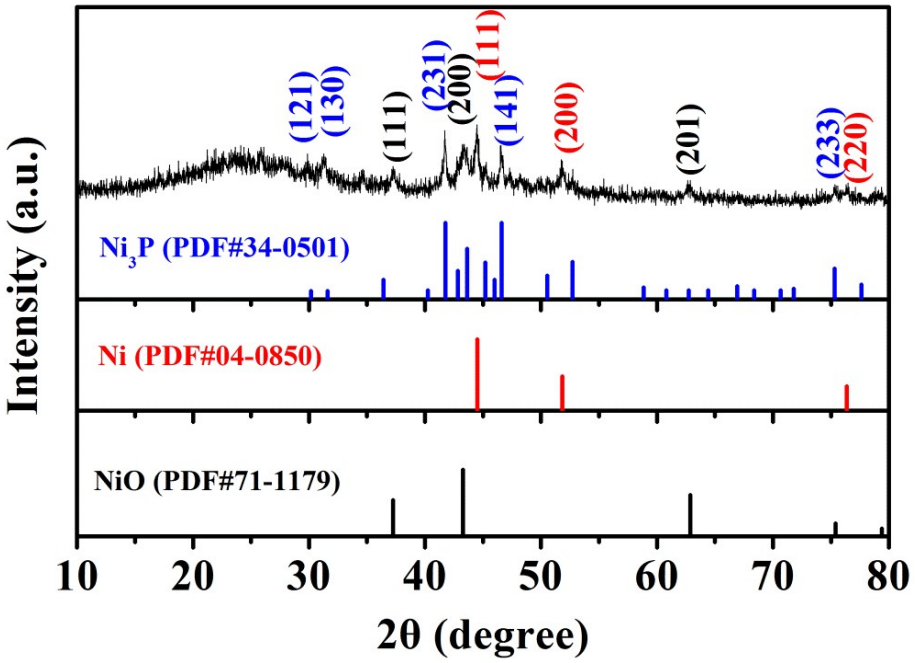

Fig. S13 XRD pattern of the as-synthesized NiP_x/NiO_x/rGO/C using Lactobacillus bulgaricus as template and phosphorous source.

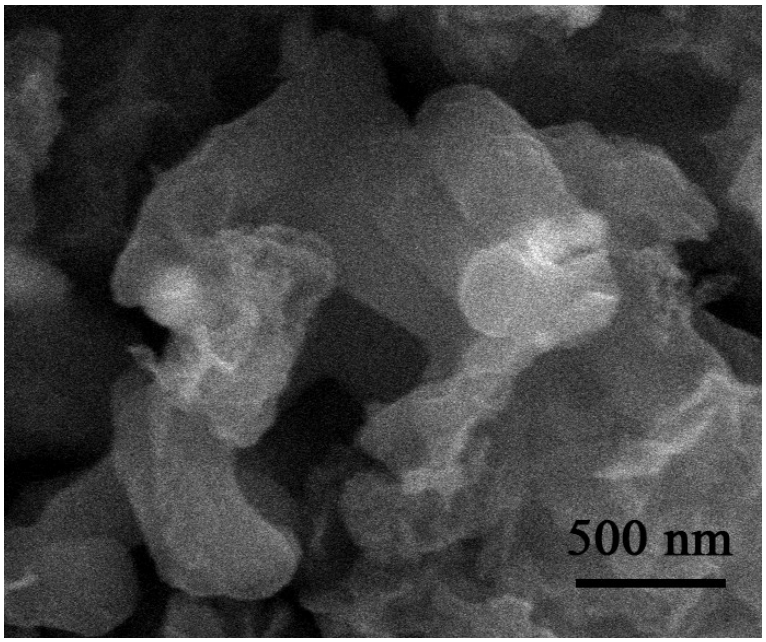

Fig. S14 SEM image of the as-synthesized NiP_x/NiO_x/rGO/C using Lactobacillus bulgaricus as template and phosphorous source.

Table S1 Simulated parameters of Nyquist plots for the ORR on Co_2P-Co_3O_4/C and Co_2P-Co_3O_4/rGO/C.

Samples	R_s[a] [Ω cm^{-2}]	CPE1[d] [Ω cm^{-2}]	n_1	R_C[b] [Ω cm^{-2}]	CPE2[e] [Ω cm^{-2}]	n_2	R_t[c] [Ω cm^{-2}]
Co_2P-Co_3O_4/C	6.83	0.021	0.47	41.16	0.004	0.87	202.6
Co_2P-Co_3O_4/rGO/C	6.66	0.145	0.40	2.36	0.007	0.92	45.18

[a]electrolyte resistance;
[b]catalyst film intrinsic resistance;
[c]charge transfer resistance for ORR;
[d,e]constant phase element.

Table S2 Performance comparison of recent works on cobalt phosphide based ORR catalysts.

Samples	Catalyst loading [mg cm^{-2}]	E_{onset} [V]	$E_{1/2}$ [V]	Tafel slope [mV dec^{-1}]	J_L [mA cm^{-2}]	Ref.
Co_2P@CNF	0.20	0.92	0.80	77.10	5.27	1
Co_2P/NPC	N/A	N/A	082	69.8	N/A	2
Co_2P NRs	N/A	N/A	0.77	N/A	4.60	3
Co_2P@CoNPG	0.20	0.90	0.81	69.0	6.68	4
HCNT-Co_2P	N/A	0.84	0.77	N/A	N/A	5
BNC/Co_2P	0.21	0.92	0.82	N/A	N/A	6
Co_xP-CNTs	N/A	0.84	0.76	N/A	N/A	7
Urchin-like CoP	0.28	0.80	0.70	51.0	4.50	8
Co/CoP-HNC	0.19	0.94	0.83	59.4	N/A	9
CoP NCs	0.20	0.92	0.86	72.1	4.64	10
Co_2P-Co_3O_4/rGO/C -800	0.20	0.91	0.80	58.2	4.96	This work

References

1. J. Gao, J. Wang, L. Zhou, X. Cai, D. Zhan, M. Hou, L. Lai, *ACS Appl. Mater. Interfaces*, 2019, **11**, 10364-10372.
2. Y. Yu, J. Ma, C. Chen, Y. Fu, Y. Wang, K. Li, Y. Liao, L. Zheng, X. Zuo, *ChemCatChem*, 2019, **11**, 1722-1731.
3. V.V.T. Doan-Nguyen, S. Zhang, E.B. Trigg, R. Agarwal, J. Li, D. Su, K.I. Winey, C.B.

Murray, *ACS Nano*, 2015, **9**, 8108-8115.

4. H. Jiang, C. Li, H. Shen, Y. Liu, W. Li, J. Li, *Electrochim. Acta*, 2017, **231**, 344-353.
5. K. Chen, X. Huang, C. Wan, H. Liu, *RSC Adv.*, 2015, **5**, 92893-92898.
6. C. Han, X. Bo, Y. Zhang, M. Li, A. Wang, L. Guo, *Chem. Commun.*, 2015, **51**, 15015-15018.
7. K. Chen, X. Huang, C. Wan, H. Liu, *Chem. Commun.*, 2015, **51**, 7891-7894.
8. H. Yang, Y. Zhang, F. Hu, Q. Wang, *Nano Lett.*, 2015, **15**, 7616-7620.
9. Y. Hao, Y. Xu, W. Liu, X. Sun, *Mater. Horiz.*, 2018, **5**, 108-115.
10. H. Li, Q. Li, P. Wen, T. B. Williams, S. Adhikari, C. Dun, C. Lu, D. Itanze, L. Jiang, D. L. Carroll, G. L. Donati, P. M. Lundin, Y. Qiu, S. M. Geyer, *Adv. Mater.*, 2018, **30**, 1705796.